Hindawi Publishing Corporation
Advances in Materials Science and Engineering
Volume 2014, Article ID 918906, 7 pages
http://dx.doi.org/10.1155/2014/918906

Research Article

Prediction of Three-Dimensional Milling Forces Based on Finite Element

Lida Zhu,[1] Chunxia Zhu,[2] Jiaying Pei,[1] Xuebing Li,[3] and Wei Wang[1]

[1] *School of Mechanical Engineering and Automation, Northeastern University, Shenyang 110819, China*
[2] *School of Traffic and Mechanical Engineering, Shenyang Jianzhu University, Shenyang 110168, China*
[3] *Liaoning Guidaojiaotong Polytechnic Institute, Shenyang, Liaoning 110023, China*

Correspondence should be addressed to Lida Zhu; zld1999@gmail.com

Received 15 April 2014; Revised 16 July 2014; Accepted 11 August 2014; Published 28 October 2014

Academic Editor: Charles C. Sorrell

The model of milling force is mainly proposed to predict and analyze the cutting process based on finite element method in this paper. Firstly, milling finite element model is given based on orthogonal cutting principle, and then the influence laws of cutting parameters on chip formation are analyzed by using different simulation parameters. In addition, the three-dimensional milling forces are obtained from finite element models. Finally, the values of milling force by the milling experiment are also compared and analyzed with the simulation values to verify the feasibility and reasonability. It can be shown that milling forces match well between simulation and experiment results, which can provide many good basic data and analysis methods to optimize the machining parameters, reduce tool wear, and improve the workpiece surface roughness and adapt to the programming strategy of high speed machining.

1. Introduction

At present, traditional processing methods almost depended on experience and processing standards. But with the rapid advancement of scientific technology, the goal of manufacturing technology produces parts correctly in the shortest time, in the lowest cost, and in the most effective way. Since the product complexities are increasing and the competitive product life cycle times are reduced, the most effective method is to develop a set of virtual simulation systems for machining process [1, 2]. It leads to the necessity that finite element method replaces physical machining process to analyze and optimize cutting parameters.

In cutting process, the relationship between inputs (cutting parameters, tool geometry and material properties, workpiece geometry and material properties, etc.) and outputs (cutting force, cutting temperature, cutting vibration, surface quality, etc.) can be obtained based on the change of processing conditions, so the processing scheme can be modified and machining parameters can be optimized depending on the simulation results [3, 4]. With the rapid development of computer technology, finite element simulation has been developed to study the mechanics of machining, optimization of cutting parameters, cutting tool design, and so forth. The ultimate goal is mainly to eliminate expensive and time consuming experimental modeling approaches in favor of simulation models that are capable of producing realistic results at practical cutting conditions in process design [5–7]. In addition, FEM permits obtaining the relation between cutting forces and chip thickness for different cutting speeds and feed rates. The influences of some important parameters include the cutting edge radius, rake angle, clearance angle, depth of cut, and cutting velocity [8–10].

There are some literature researches on this finite element method in cutting process. Aurich and Bil [11] have presented a 3D coupled finite element model for the simulation of segmented chip formation in metal cutting. The generation of segmentation is achieved by element erase with respect to damage or by modification of material flow stress data. Özel et al. [12] have proposed that the modified material models with strain softening effect are developed to simulate chip formation with finite element analysis and investigate

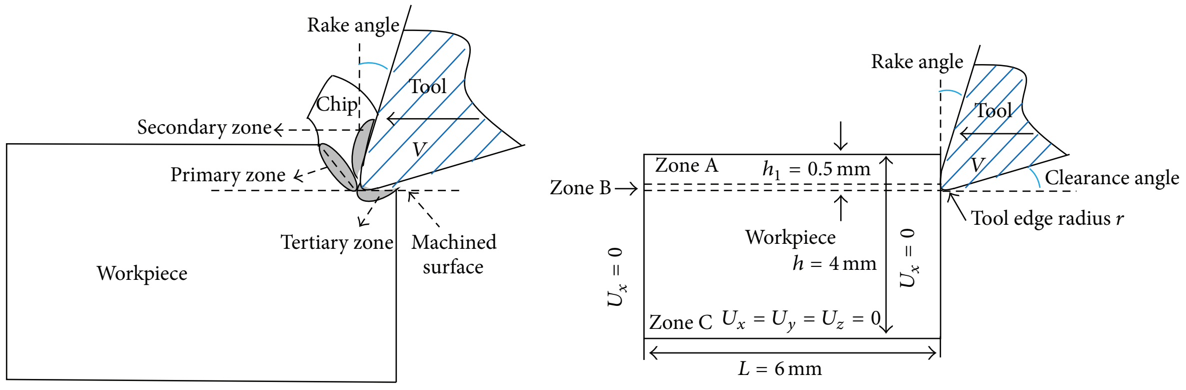

(a) (b)

FIGURE 1: (a) Orthogonal cutting configuration. (b) Decomposition of the workpiece in different zones A, B, and C.

temperature fields for coated inserts. Predicted forces and tool wear contours are compared with experiments. Bouzakis et al. [13] have presented an integrated procedure for simulating the complicated chip formation. The developed FEM model capabilities have been demonstrated in terms of chip flow and morphology in cutting of spur gears as well as in the four possible cutting variations of helical gears. Yen et al. [14] have studied estimation of tool wear in orthogonal cutting using the finite element analysis. Based on temperatures and stresses on the tool face predicted by the finite element analysis simulation, tool wear may be estimated with acceptable accuracy using an empirical wear model. Therefore, it is feasible and rational that finite element method can be instead of traditional experimental method by the comparisons of milling force in simulation and experiment conditions.

Henceforth this paper is organized as follows. Section 2 briefly describes modeling of orthogonal cutting based on finite element and Johnson-Cook material model. In Section 3, a detailed study of chip formation and cutting forces and the comparison of milling forces are analyzed in simulation and experimental process. In Section 4, some conclusions from this study are given.

2. Modeling of Orthogonal Cutting Based on Finite Element

In orthogonal cutting, the material is removed by a cutting edge that is perpendicular to the direction of relative tool-workpiece motion. The orthogonal cutting resembles a shaping process with a straight tool and a metal chip is sheared away from the workpiece. As the edge of tool penetrates into the workpiece, the material ahead of tool is sheared over the primary shear zone to form a chip. The chip partially deforms and moves along the rake face of the tool, which is called the secondary deformation zone. The friction area, where the flank of tool rubs the newly machined surface, is called the tertiary zone [1]. The chip leaves the tool, losing contact with the rake face of the tool, and the length of contact zone depends on the cutting speed, tool geometry, and material properties. In orthogonal milling, the cutting is assumed to be uniform along the cutting edge; therefore it is a two-dimensional plane strain deformation process without side spreading of the material. Hence, the cutting forces are exerted in the directions of velocity and uncut chip thickness, which are called feed forces and tangential forces [1, 4]. The 2D orthogonal cutting configuration and contact zone in two-dimensional plane are shown in Figure 1(a).

The FE orthogonal cutting model was created by using the 3D DEFORM software with Lagrangian formulation, which means material is attached to the mesh, with periodic remeshing to avoid severe element distortion. The cutting process requires a coupled thermomechanical analysis, because mechanical work is converted into heat, causing thermal strains and influencing the material properties [15]. The basic geometry of the numerical model and decomposition zone is shown and simplified into 2D cutting model in Figure 2(b). According to the assumption, a plane strain finite element model based on an updated Lagrangian approach is presented. The wokrpiece is fixed at the lowest contour and the cutting speed is applied to the tool. The mesh of the workpiece is divided into three different zones. The layer of material which will be removed by cutting is composed of zone A (main part) and zone B (thin bottom layer of $10\,\mu$m thickness). The upper limit of zone C corresponds to the machined surface. The mesh at zone B and zone C is parallel to horizontal and vertical directions, wherein zone B is an important part, so its meshed element density is more than other parts, while the mesh at zone A is characterized by an inclination angle with the horizontal direction. A sensitivity analysis is conducted so that the number of elements in the mesh is large enough, so the workpiece mesh does not influence the prediction obtained with the FE simulations. Therefore, the orientation of the mesh is aimed at facilitating the formation of segmented chip.

The tool is assumed to be rigid and workpiece material is taken as isotropic, elastic-viscoplastic in the model. The workpiece consists of four-node isoparametric quadrilateral plane strain coupled elements. The cutting condition (cutting

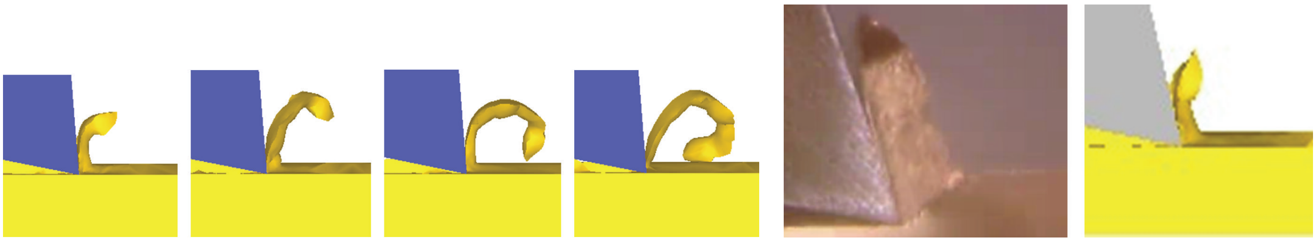

(a) Chip formation process in different steps

(b) Comparison of chip formation between simulation and experiment (rake angle 15°)

Rake angle 5°

Rake angle 10°

Rake angle 20°

$V = 20\,\mathrm{m/min}$

$V = 40\,\mathrm{m/min}$

$V = 80\,\mathrm{m/min}$

(c) Shape of chips in different rake angles

(d) Shape of chips in different cutting speeds

FIGURE 2: Shape of chips in different cutting condition.

speed V, uncut chip thickness h_1, rake angle, and tool edge radius r; see Figure 1(b)) depends also on the physical and mechanical properties of the work-material during machining, such as mass density and parameters of the Johnson-Cool law from (1). The simple formulation is adopted here, frequently used for numerical simulations of machining. Therefore, the Johnson-Cook (JC) material model is widely used for analysis of material flow stress, especially for those materials of which their flow stress is highly influenced by temperature and strain rate; the influence of stain, strain rate, and temperature on the flow stress is defined by three multiplicative yet distinctive terms [14–16]:

$$\sigma = \left(\mathrm{A} + \mathrm{B}\varepsilon^{n}\right)\left(1 + \mathrm{C}\ \ln\frac{\dot{\varepsilon}}{\dot{\varepsilon}_0}\right)\left[1 - \left(\frac{T - T_r}{T_m - T_r}\right)^{m}\right], \qquad (1)$$

where σ is the equivalent flow stress, ε is the equivalent plastic strain, $\dot{\varepsilon}$ is the equivalent plastic strain rate, $\dot{\varepsilon}_0$ is the reference equivalent plastic strain, T is the workpiece temperature, T_m is the material melting temperature, T_r is the room temperature, and other letters are related to workpiece material from experiment measure.

For the continuous chip, the relation between cutting force F and shear stress τ in the shear plane (shear band for the serrated chip formation) can be obtained in stable mechanical equilibrium [1, 15]; that is,

$$F = \tau \cdot b\omega \frac{\cos\left(\beta - \omega\right)}{\cos\left(\varphi + \beta - \omega\right) \cdot \sin\varphi}, \qquad (2)$$

where b is the uncut chip thickness, φ shear angle, ω the cutting width, and β the tool-chip friction angle. It can be seen from (1) that the cutting force is approximately in proportion to the shear stress in the shear band.

3. Comparison of Milling Forces between Simulation and Experiment

3.1. Simulation of Chip Formation and Milling Forces. The FE chip formation model was created by using updated Lagrangian formulation, in which the material is attached to the mesh, with periodic remeshing to avoid severe element distortion. Three-dimensional simulation is conducted by DEFORM software on the aspects of mesh generation and material removal, so that it is better to realize the chip separation. With the dynamic adaptation grid technology which avoids the mesh distortion and improves the accuracy of the solving, the simulation results can be more reliable by the Lagrangian method [16]. The chip formation is shown in different steps in Figure 2(a). Because the formation of chip is the result of the deformation of workpiece material (aluminum 2A12), it does not need to have a chip separation criterion. The comparison of chip formation between simulation and experiment is shown in Figure 2(b). The shapes of chip in different rake angles and in different cutting speeds are shown, respectively, in Figures 2(c) and 2(b).

Three-dimensional milling forces are simulated based on chip formation in different cutting parameters. Aluminum 2A12 is used as workpiece material. There are two cutting conditions as follows: cutting speed 125 m/min, cutting depth 4 mm, feed 100 mm/min, and cutting forces are shown in x, y, and z direction in Figure 3 and other cutting conditions, cutting speed 125 m/min, cutting depth 8 mm, feed 100 mm/min, cutting forces, are shown in x, y, and z direction in Figure 4. It can be noticed in Figures 3 and 4 that load predictions can be measured in milling process, and then the average values are calculated and obtained based on these data. Therefore, the milling force is 690 N in x direction, 748 N in y direction, and 103 N in z direction, as shown in Figure 3. The milling

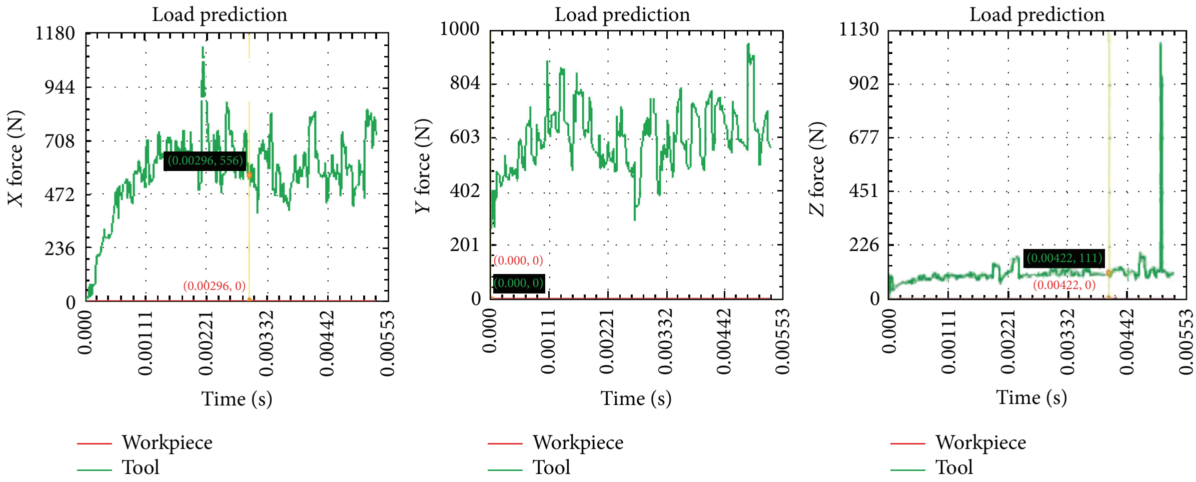

Figure 3: Simulation results of milling forces in x, y, and z directions.

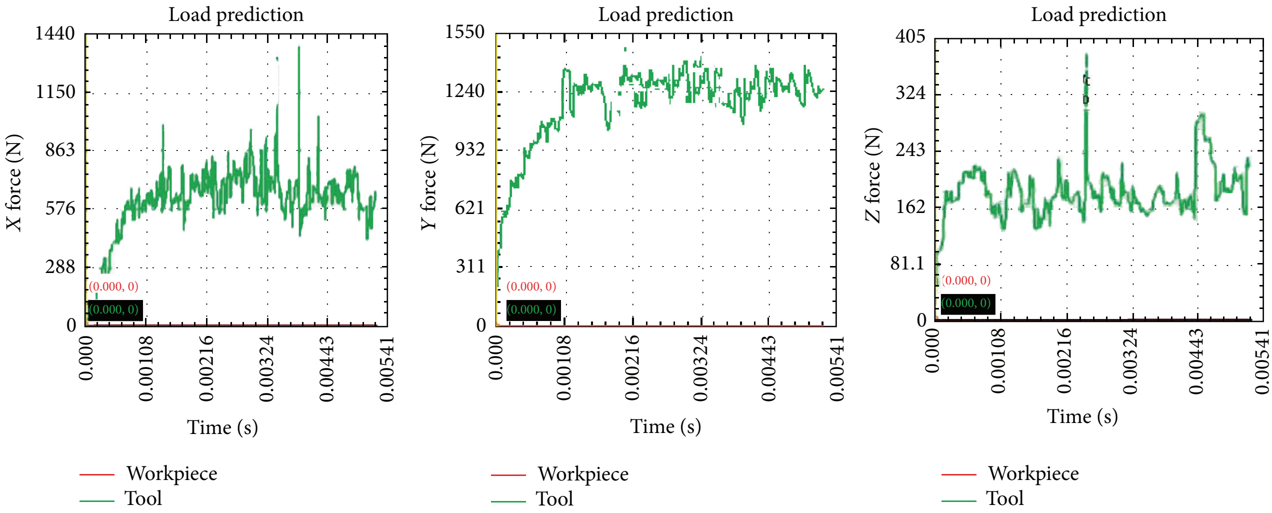

Figure 4: Simulation results of milling forces in x, y, and z directions.

force is 651 N in x direction, 1202 N in y direction, and 174 N in z direction, as shown in Figure 4.

3.2. Milling Forces Analysis and Validation. Milling experiments should be carried out to verify the currency of the values got from the finite element simulation. The milling test was conducted in vertical milling centre (TH5650) in Figure 5, and cutting tool used in turn-milling test was 20 mm diameter end mill (TAP300R-2020-160-H.) equipped with four inserts and a tool holder (SBT40-MLK32-105) made by CHAIN HEADWAY Inc. The insert for MITSUBISHI used is APMT1135PDER-M0, which is LC15TF coated. The insert itself is a rhombic shaped end milling insert with a cutting edge length of 11 mm, a width of 6.35 mm, and a 0.2 mm corner radius.

The kind of aluminum alloy (2A12) is a precipitation hardening aluminum alloy, containing magnesium and silicon as its major alloying elements. It is one of the most common alloys of aluminum for general purpose use, which has good mechanical properties and exhibits good weldability. And a wide variety of applications such as aircraft fittings, camera lens mounts, couplings, marines fittings, electrical

Figure 5: Vertical milling machining centre (TH5650) and dynamometer.

Table 1: Chemical composition of 2A12 aluminum alloy (mass fraction, %).

Cu	Mg	Mn	Fe	Si	Zn	Ni	Ti	Al
4.52	1.62	0.58	0.28	0.16	<0.20	0.10	0.10	Others

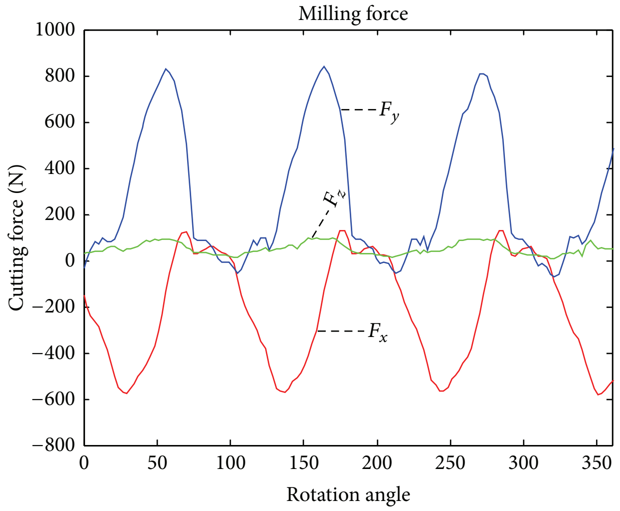

Figure 6: Cutting force in $x/y/z$ direction (cutting speed 125 m/min, cutting depth 4 mm, and the feed 100 mm/min).

fittings, hydraulic pistons and appliance fittings. Chemical composition of 2A12 aluminum alloy is shown in Table 1.

For measuring the cutting forces in x, y, and z direction, the Kistler9257B dynamometer is mounted on the machining center. In the down milling, cooling method is dry cutting. In order to compare the milling forces between simulation and experiment, the cutting condition and experimental results of cutting forces are shown in Figures 6 and 7.

The comparison value of experimental results and simulation results in x, y, and z directions is shown in Table 2.

It can be seen in Table 2 that milling forces are matched between simulation and experiment, and the finite element method is feasible and effective in replacing the traditional experimental method with finite element simulation. But there are some errors between simulation experiments; in particular the milling forces in z direction result from some factors are neglected in simulation process. Firstly, the model of milling cutter is simplified and regarded as rigid in ideal condition, which will have effect on the milling forces. In addition, since the limitation of computer performance and parameters of workpiece material, it will lead to the errors of milling forces between simulation and experiment.

The influence laws of cutting parameters on cutting force and cutting efficiency are studied based on finite element model, wherein cutting efficiency is a reasonable index in more than 500 mm^3/min range [16]. So the influence laws are obtained in cutting speed, depth of cut, and the feed, respectively, as shown in Figure 8.

It can be noticed that cutting forces are small when the cutting parameter is small; at the same time, cutting efficiency is very low, which is not in the reasonable range and cannot meet the needs of actual production. With the increase of depth of cut and feed, cutting efficiency and the cutting force gradually increase. But with the increase of cutting speed, cutting force can decrease and the cutting efficiency is very high. As a result, the increase of cutting speed can realize the optimization of tool life and the production efficiency.

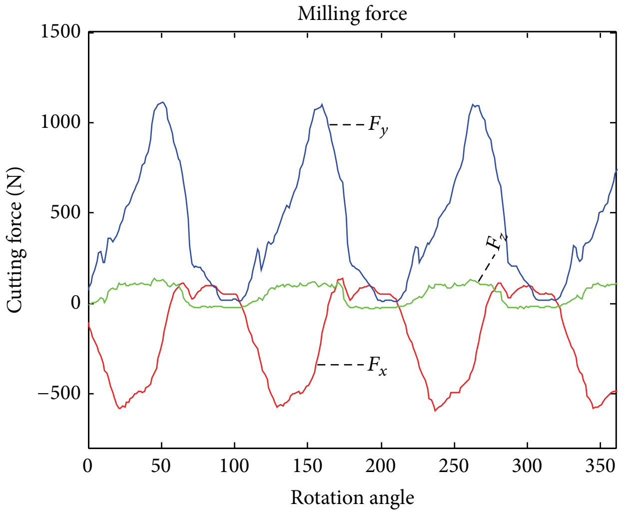

Figure 7: Cutting force in $x/y/z$ direction (cutting speed 125 m/min, cutting depth 8 mm, and the feed 100 mm/min).

4. Conclusions

(1) The model of three-dimensional cutting force is proposed to predict and analyze chip formation and milling force based on finite element method. The influence laws of cutting parameters on chips and milling forces are obtained in milling process. The comparison of milling forces in simulation and experiment values is analyzed to verify the feasibility based on finite element method.

(2) With the increase of rake angle, the chip shape becomes thin and long. Cutting speed increases much, the curling radius of chip becomes smaller, and at the same time, cutting force can decrease and cutting efficiency is very high, which can realize the optimization of tool life and the production efficiency.

(3) Some factors are neglected in the simulation process, so they lead to some errors between experiment and simulation. In addition, the model of milling cutter is simplified, so that there are some differences compared with the real milling cutter. In the simulation process, the cutter is in ideal condition, which the cutter is regarded as a rigid model and not considered the existing friction and vibration, but in the real cutting process, there is some wear existing on the milling cutter, which may affect the critical value of cutting force.

Table 2: Comparison of cutting forces between simulation and experiment.

1	Experimental values	Simulation values	Error values	2	Experimental values	Simulation values	Error values
F_x	579	690	1.90%	F_x	598	651	8.66%
F_y	826	748	9.44%	F_y	1116	1202	7.71%
F_z	97.2	103	5.97%	F_z	157	174	10.8%

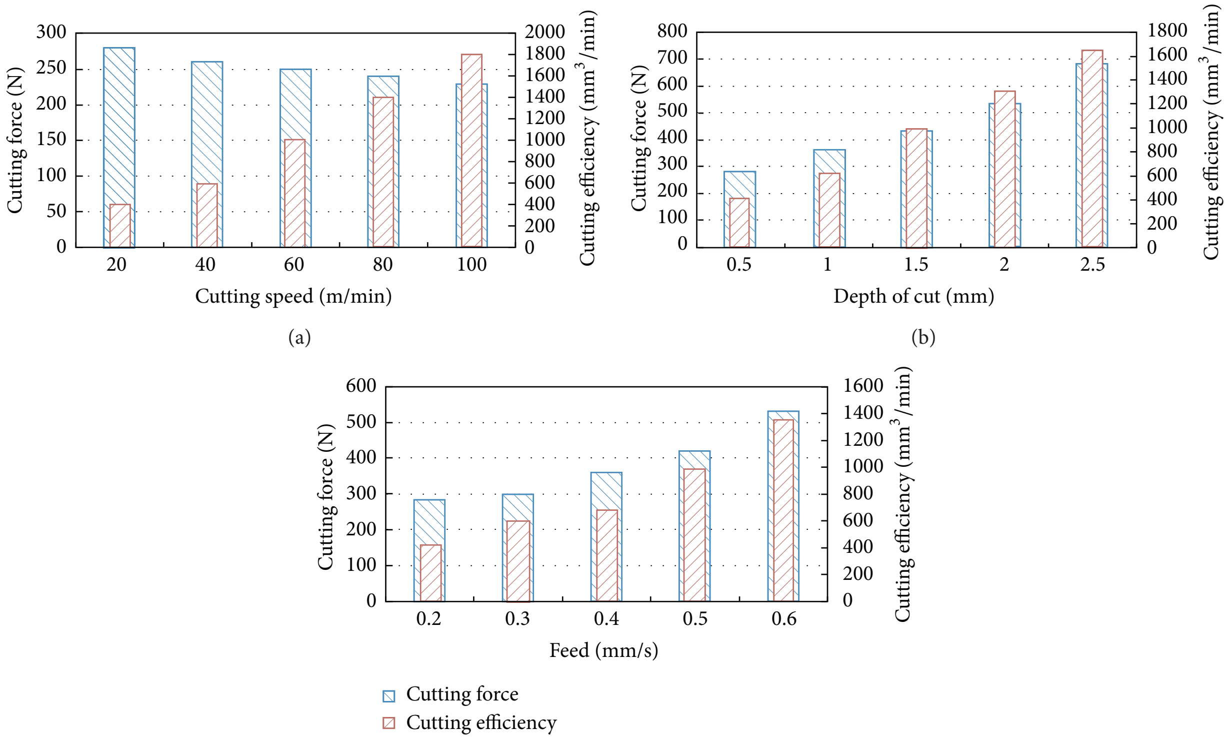

(a)

(b)

(c)

Figure 8: (a) Cutting force and cutting efficiency contrast in different cutting speed (cutting depth 0.5 mm; feed 0.2 mm/s). (b) Cutting force and cutting efficiency contrast in different depth of cut (cutting speed 20 mm/min; feed 0.2 mm/s). (c) Cutting force and cutting efficiency contrast in different feed (cutting speed 20 mm/min; cutting depth 0.5 mm).

Conflict of Interests

The authors declare that there is no conflict of interests regarding the publication of this paper.

Acknowledgments

This work was supported by National Natural Science Foundation of China (NSFC) (51105072 and 51475087) and Fundamental Research Funds for the Central Universities (N130403010).

References

[1] Y. Altintas, Manufacturing Automation-Metal Cutting Mechanics, Machine Tool Vibrations, and CNC Design, The University of British Columbia, 2000 and 2012.

[2] Y. Altintas, C. Brecher, M. Week, and S. Witt, "Virtual machine tool," *CIRP Annals—Manufacturing Technology*, vol. 54, no. 2, pp. 115–138, 2005.

[3] R. Jingkui, K. Yinglin, and Y. Yong, "Finite element simulation of serrated chip formation in high-speed milling of alloy cast iron," *Tool Engineering*, vol. 40, no. 4, pp. 40–43, 2006.

[4] G. Miao, L. Hongbin, and W. Ruijie, "The finite element simulation of effects of cutting speed and feed on milling force in high speed milling," *Tool Engineering*, vol. 44, no. 4, pp. 29–31, 2010.

[5] J. Hua and R. Shivpuri, "Prediction of chip morphology and segmentation during the machining of titanium alloys," *Journal of Materials Processing Technology*, vol. 150, no. 1-2, pp. 124–133, 2004.

[6] P. Kersting and D. Biermann, "Modeling techniques for the prediction of workpiece deflections in NC milling," *Procedia CIRP*, vol. 2, pp. 83–86, 2012.

[7] S. Seguy, G. Dessein, and L. Arnaud, "Surface roughness variation of thin wall milling, related to modal interactions," *International Journal of Machine Tools and Manufacture*, vol. 48, no. 3-4, pp. 261–274, 2008.

[8] J. P. Choi and S. J. Lee, "Efficient chip breaker design by predicting the chip breaking performance," *International Journal of*

Advanced Manufacturing Technology, vol. 17, no. 7, pp. 489–497, 2001.

[9] M. Calamaz, D. Coupard, and F. Girot, "A new material model for 2D numerical simulation of serrated chip formation when machining titanium alloy Ti-6Al-4V," *International Journal of Machine Tools and Manufacture*, vol. 48, no. 3-4, pp. 275–288, 2008.

[10] S. Sun, M. Brandt, and M. S. Dargusch, "Characteristics of cutting forces and chip formation in machining of titanium alloys," *International Journal of Machine Tools and Manufacture*, vol. 49, no. 7-8, pp. 561–568, 2009.

[11] J. C. Aurich and H. Bil, "3D finite element modelling of segmented chip formation," *CIRP Annals: Manufacturing Technology*, vol. 55, no. 1, pp. 47–50, 2006.

[12] T. Özel, M. Sima, A. K. Srivastava, and B. Kaftanoglu, "Investigations on the effects of multi-layered coated inserts in machining Ti-6Al-4V alloy with experiments and finite element simulations," *CIRP Annals—Manufacturing Technology*, vol. 59, no. 1, pp. 77–82, 2010.

[13] K.-D. Bouzakis, O. Friderikos, and I. Tsiafis, "FEM-supported simulation of chip formation and flow in gear hobbing of spur and helical gears," *CIRP Journal of Manufacturing Science and Technology*, vol. 1, no. 1, pp. 18–26, 2008, http://ithaki.meng.auth.gr/data/ICMEN2008PDF/00-PL01.pdf.

[14] Y.-C. Yen, J. Söhner, B. Lilly, and T. Altan, "Estimation of tool wear in orthogonal cutting using the finite element analysis," *Journal of Materials Processing Technology*, vol. 146, no. 1, pp. 82–91, 2004.

[15] A. Molinari, X. Soldani, and M. H. Miguélez, "Adiabatic shear banding and scaling laws in chip formation with application to cutting of Ti-6Al-4V," *Journal of the Mechanics and Physics of Solids*, vol. 61, no. 11, pp. 2331–2359, 2013.

[16] J. Pei, *Research on Physical Simulation in Cutting Process and Technical Parameters Optimization*, Northeastern University, Shenyang, China, 2011, (Chinese).


Journal of Nanotechnology

International Journal of Corrosion

International Journal of Polymer Science

Smart Materials Research

Journal of Composites

BioMed Research International

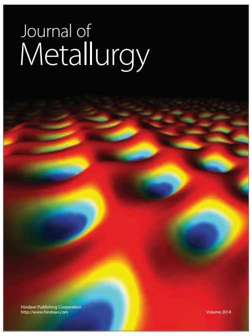
Journal of Metallurgy

Journal of Materials
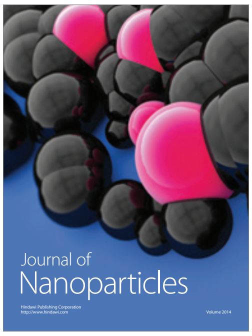
Journal of Nanoparticles
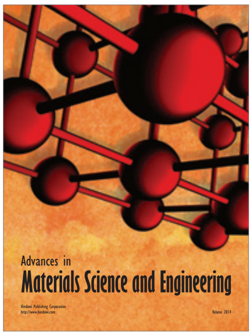
Advances in Materials Science and Engineering
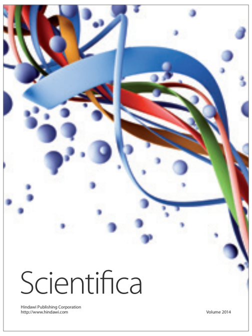
Scientifica
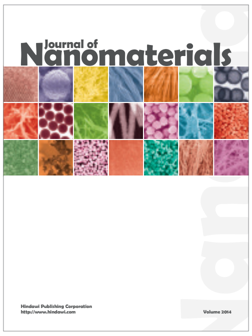
Journal of Nanomaterials

The Scientific World Journal

International Journal of Biomaterials
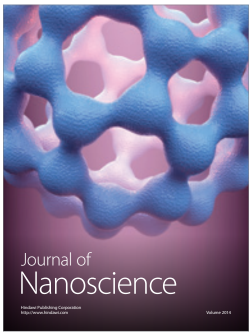
Journal of Nanoscience

Journal of Coatings
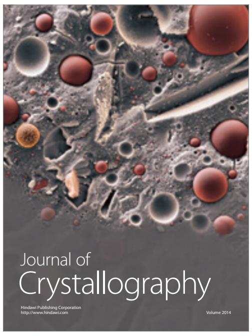
Journal of Crystallography

Journal of Ceramics

Journal of Textiles